Supplement of Atmos. Chem. Phys., 21, 14471–14492, 2021
https://doi.org/10.5194/acp-21-14471-2021-supplement

Atmospheric Chemistry and Physics
Open Access
EGU

Supplement of

Measurement report: Receptor modeling for source identification of urban fine and coarse particulate matter using hourly elemental composition

Magdalena Reizer et al.

Correspondence to: Magdalena Reizer (magdalena.reizer@pw.edu.pl)

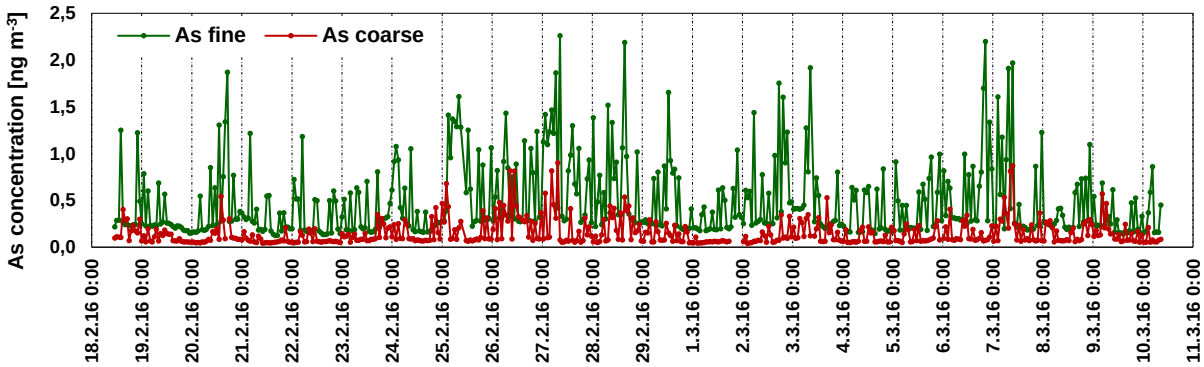

Figure S1: Hourly concentrations (ng m^{-3}) of As measured in the fine (green) and coarse (red) fractions.

15

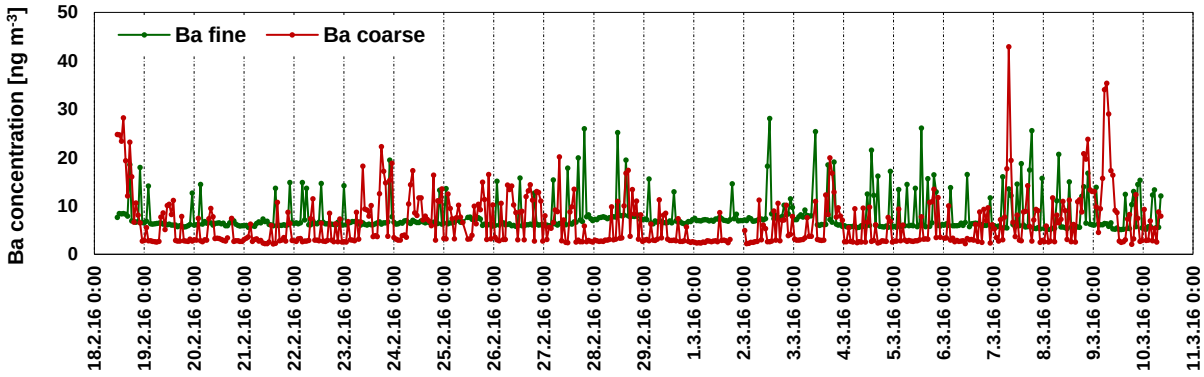

Figure S2: Hourly concentrations (ng m^{-3}) of Ba measured in the fine (green) and coarse (red) fractions.

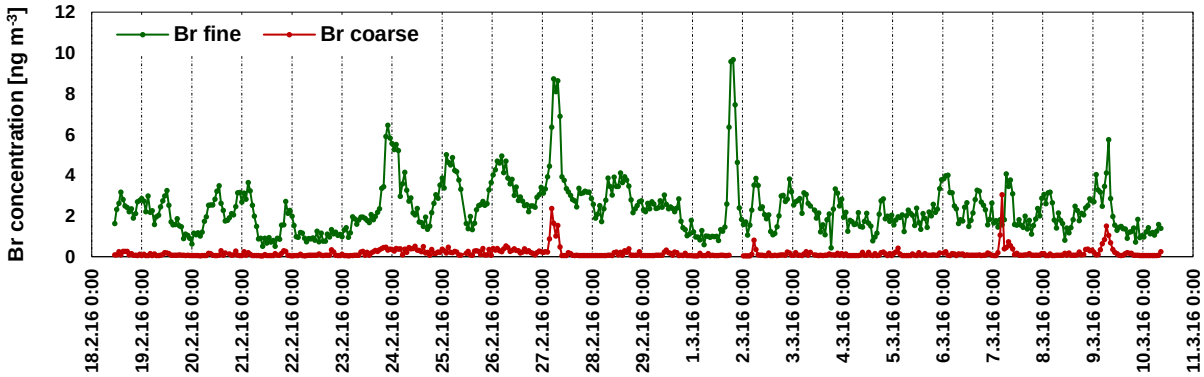

20 **Figure S3: Hourly concentrations (ng m^{-3}) of Br measured in the fine (green) and coarse (red) fractions.**

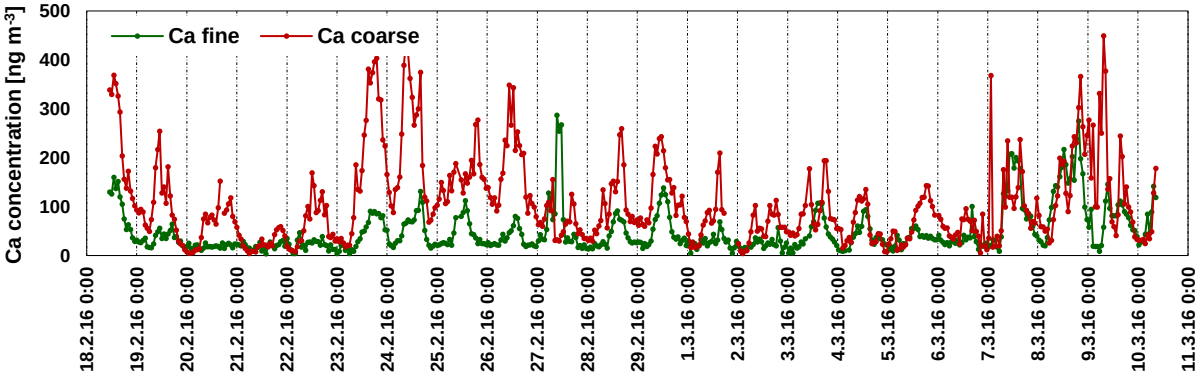

Figure S4: Hourly concentrations (ng m^{-3}) of Ca measured in the fine (green) and coarse (red) fractions.

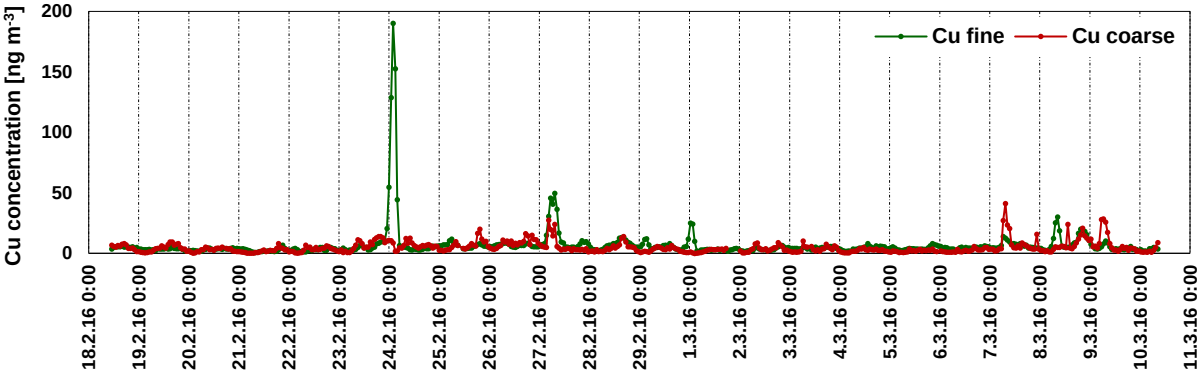

Figure S5: Hourly concentrations (ng m^{-3}) of Cu measured in the fine (green) and coarse (red) fractions.

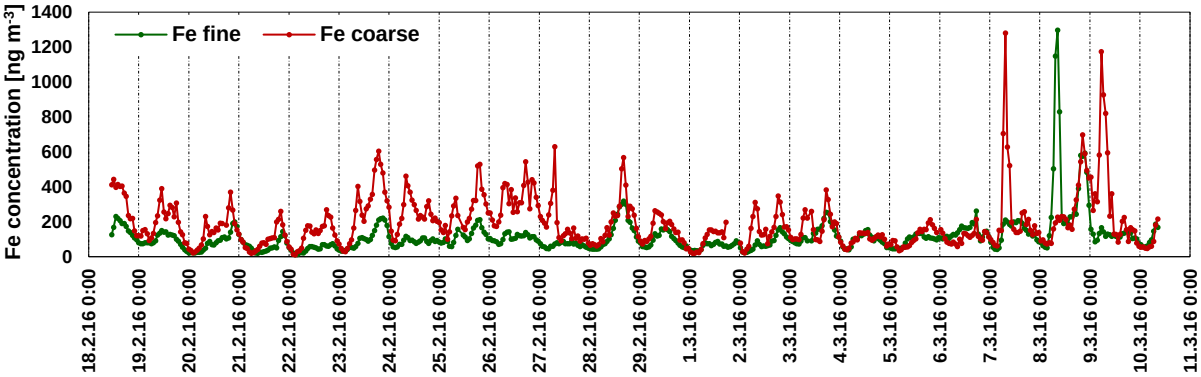

Figure S6: Hourly concentrations (ng m^{-3}) of Fe measured in the fine (green) and coarse (red) fractions.

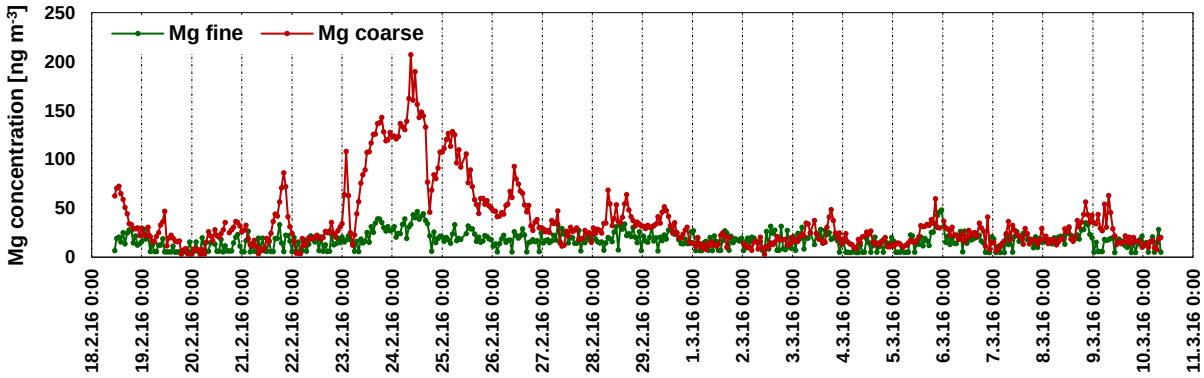

Figure S7: Hourly concentrations (ng m^{-3}) of Mg measured in the fine (green) and coarse (red) fractions.

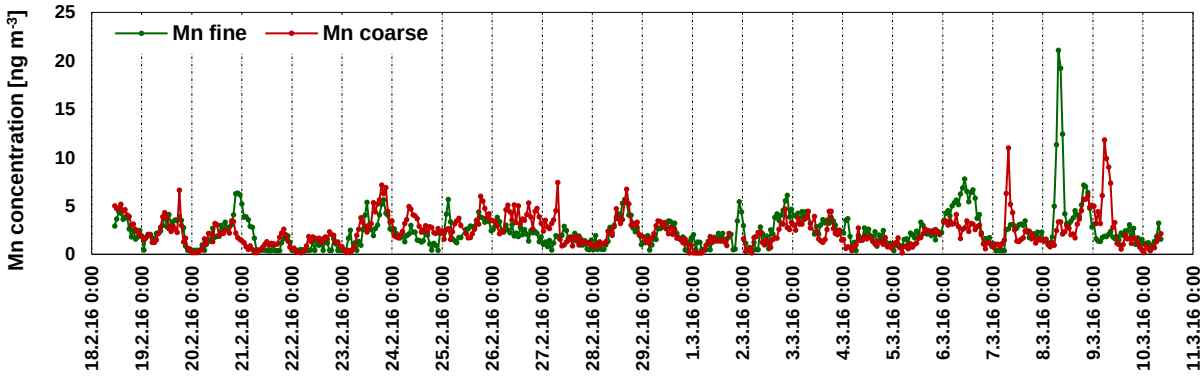

40

Figure S8: Hourly concentrations (ng m^{-3}) of Mn measured in the fine (green) and coarse (red) fractions.

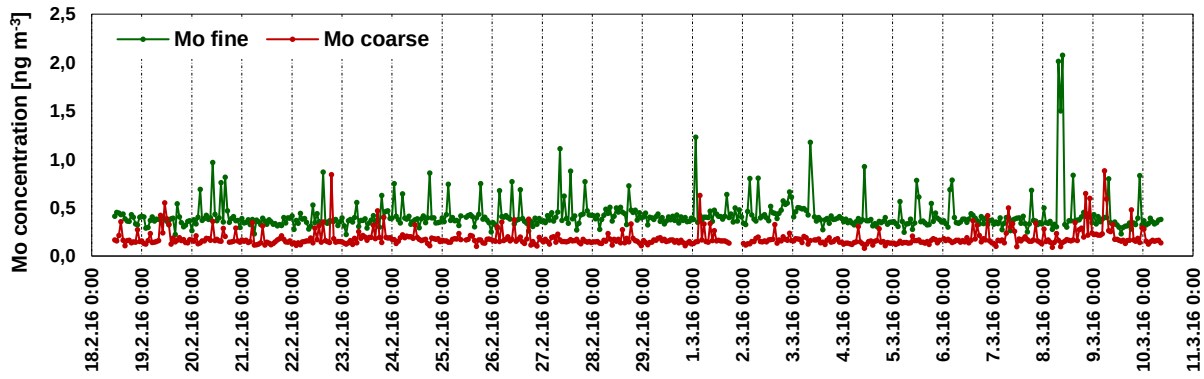

Figure S9: Hourly concentrations (ng m^{-3}) of Mo measured in the fine (green) and coarse (red) fractions.

45

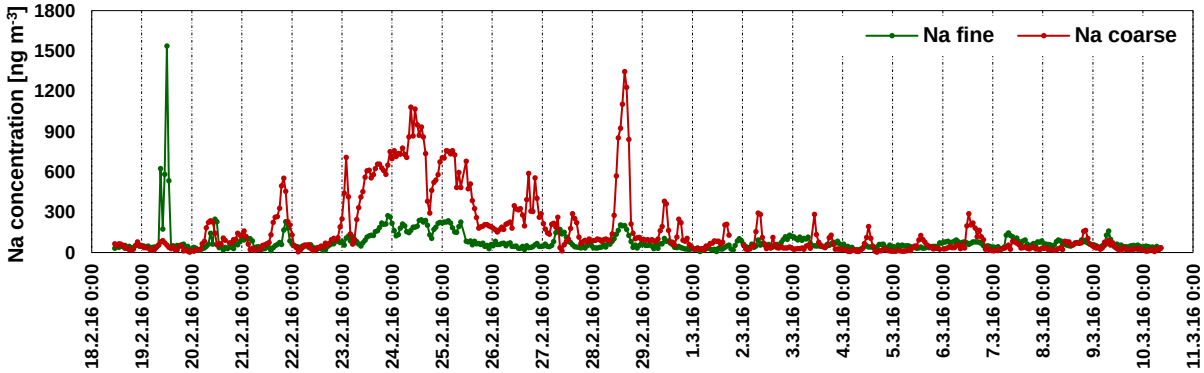

Figure S10: Hourly concentrations (ng m^{-3}) of Na measured in the fine (green) and coarse (red) fractions.

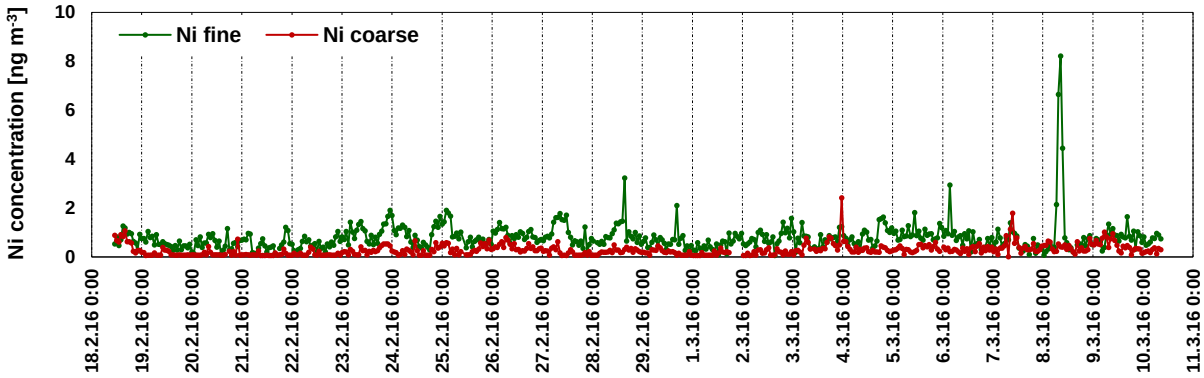

Figure S11: Hourly concentrations (ng m^{-3}) of Ni measured in the fine (green) and coarse (red) fractions.

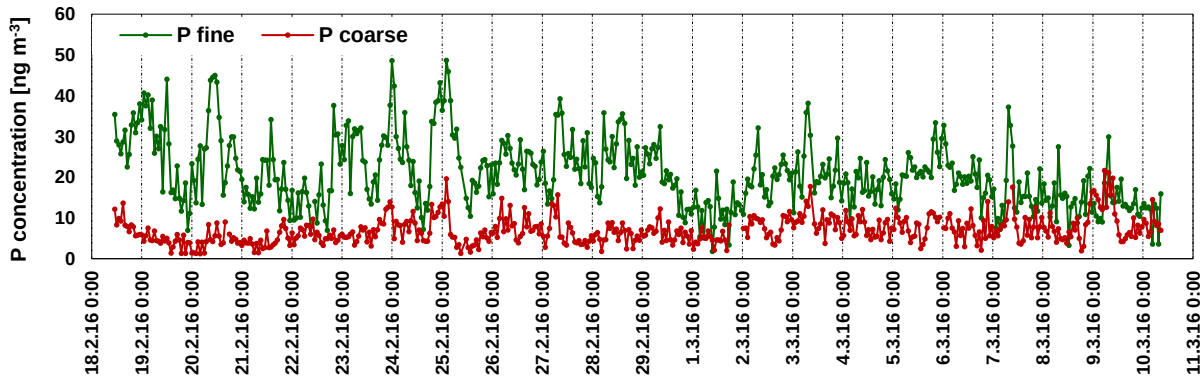

Figure S12: Hourly concentrations (ng m^{-3}) of P measured in the fine (green) and coarse (red) fractions.

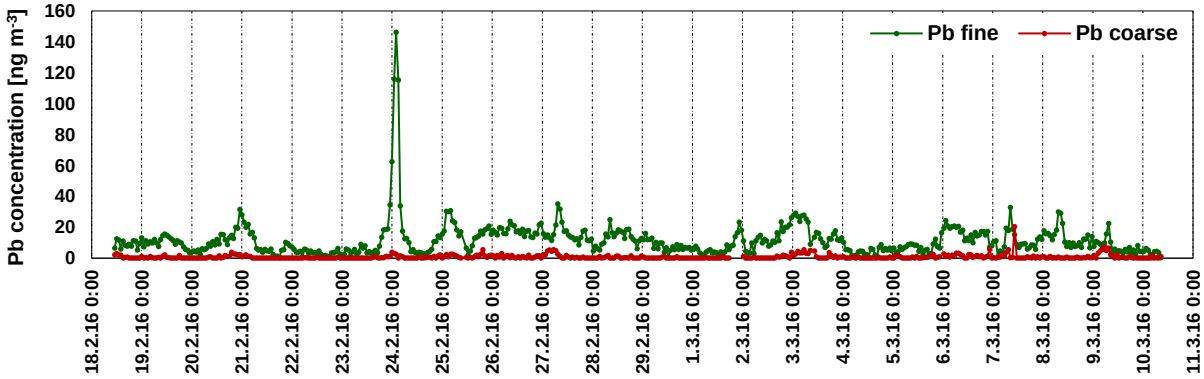

Figure S13: Hourly concentrations (ng m^{-3}) of Pb measured in the fine (green) and coarse (red) fractions.

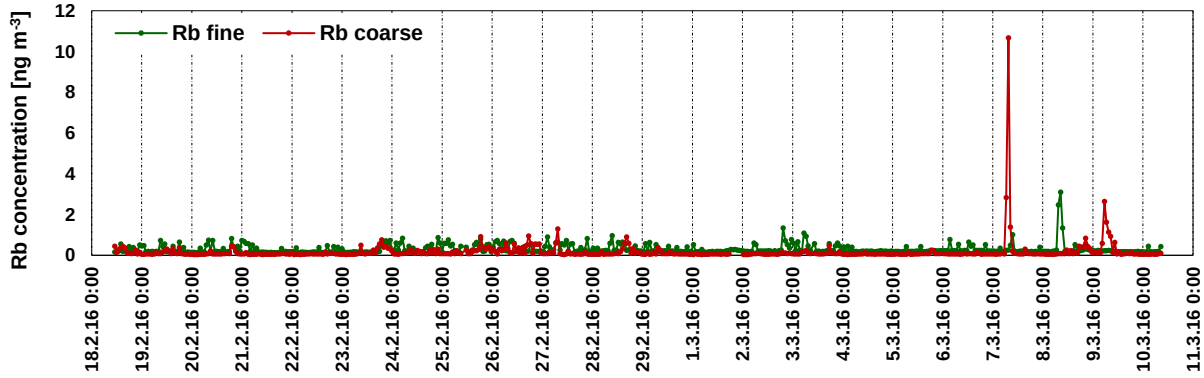

Figure S14: Hourly concentrations (ng m^{-3}) of Rb measured in the fine (green) and coarse (red) fractions.

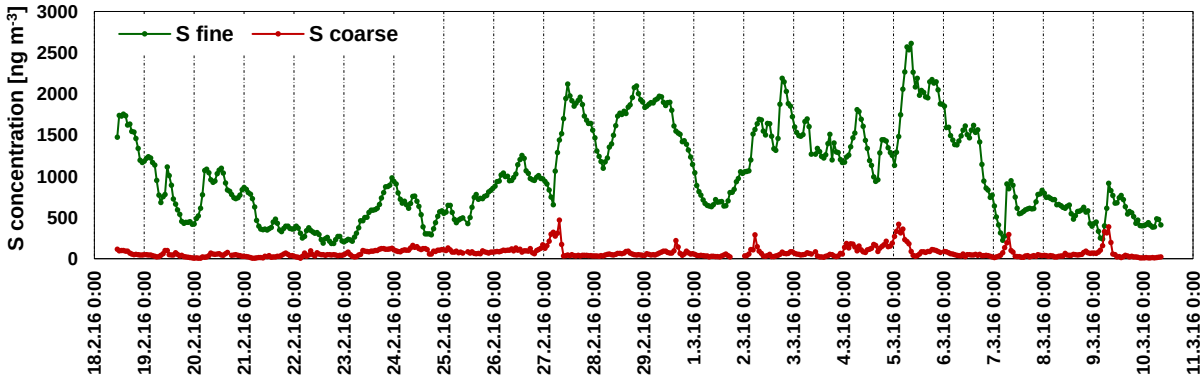

Figure S15: Hourly concentrations (ng m^{-3}) of S measured in the fine (green) and coarse (red) fractions.

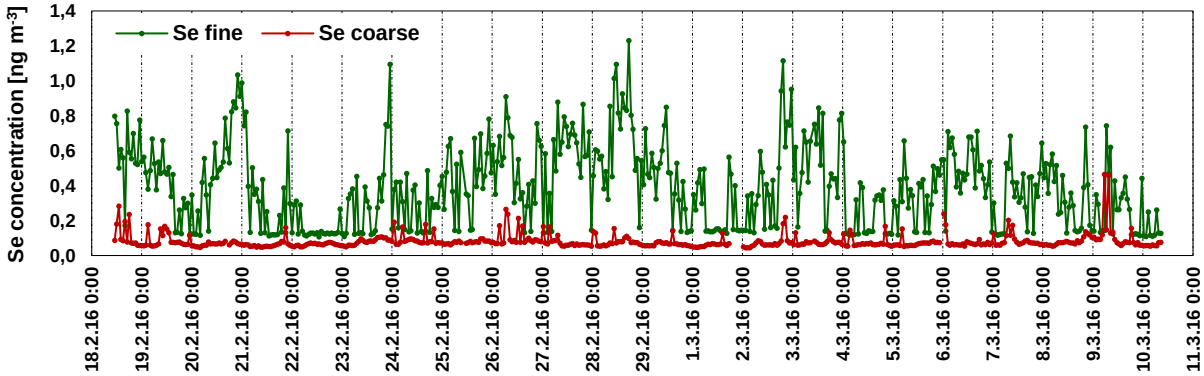

Figure S16: Hourly concentrations (ng m^{-3}) of Se measured in the fine (green) and coarse (red) fractions.

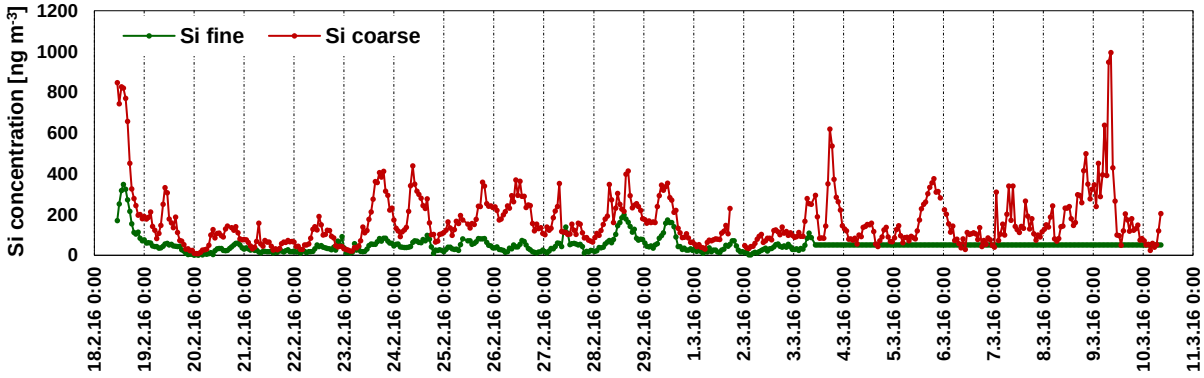

Figure S17: Hourly concentrations (ng m^{-3}) of Si measured in the fine (green) and coarse (red) fractions.

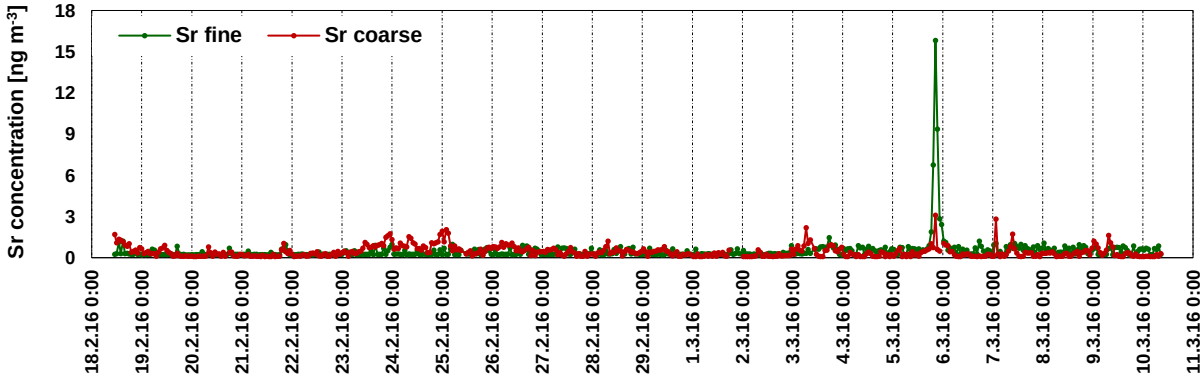

Figure S18: Hourly concentrations (ng m^{-3}) of Sr measured in the fine (green) and coarse (red) fractions.

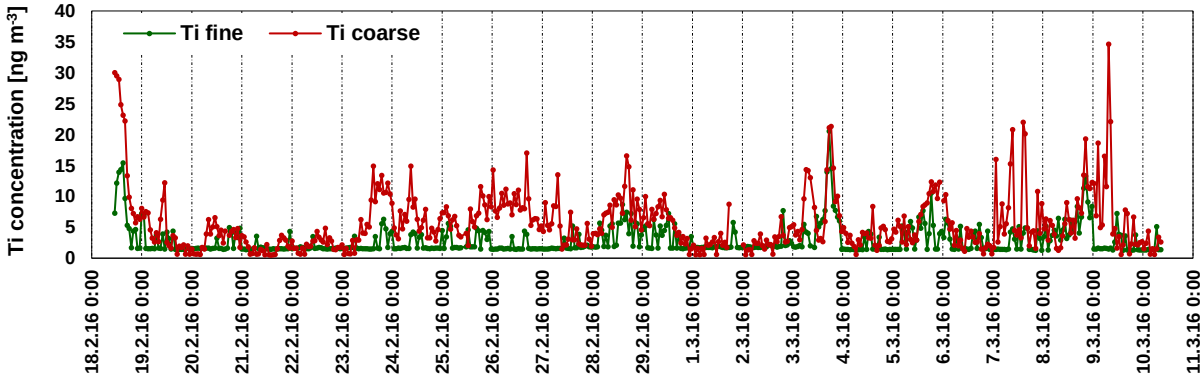

Figure S19: Hourly concentrations (ng m^{-3}) of Ti measured in the fine (green) and coarse (red) fractions.

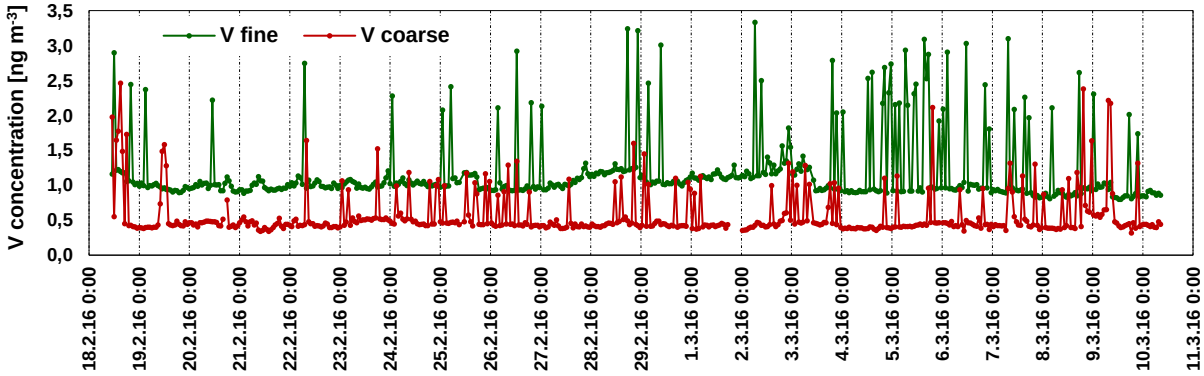

Figure S20: Hourly concentrations (ng m^{-3}) of V measured in the fine (green) and coarse (red) fractions.

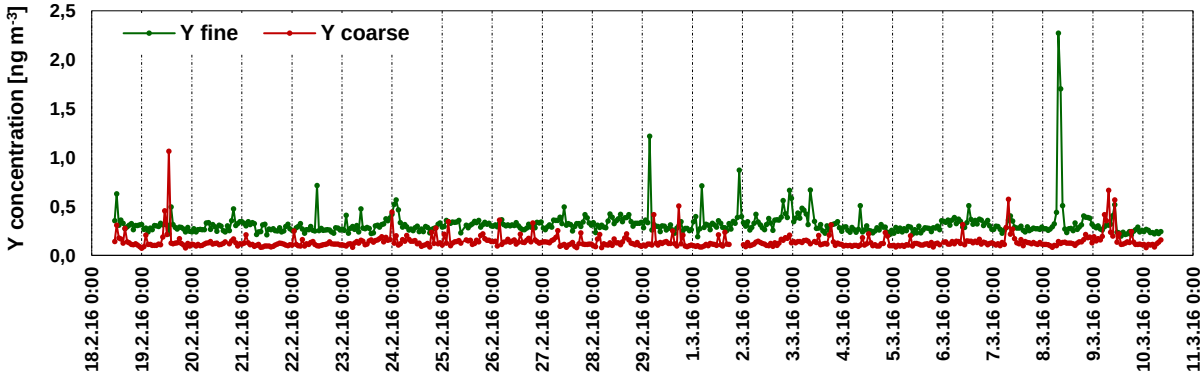

Figure S21: Hourly concentrations (ng m^{-3}) of Y measured in the fine (green) and coarse (red) fractions.

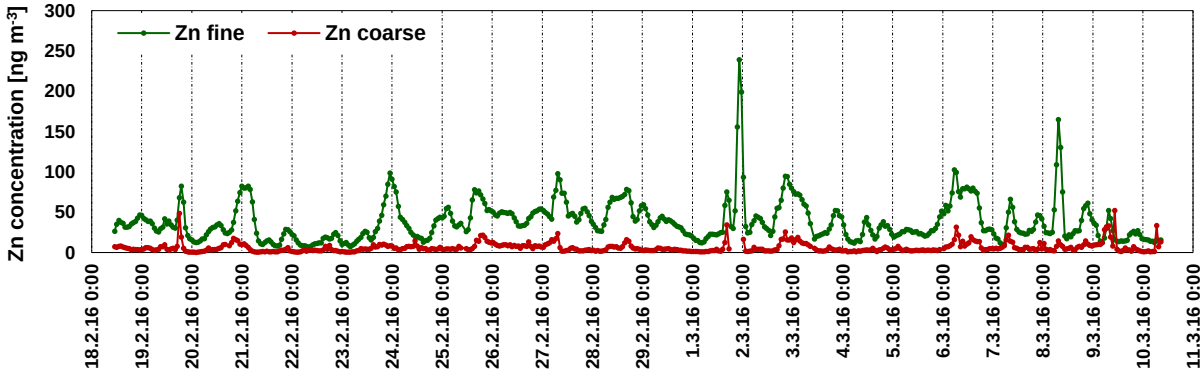

Figure S22: Hourly concentrations (ng m^{-3}) of Zn measured in the fine (green) and coarse (red) fractions.

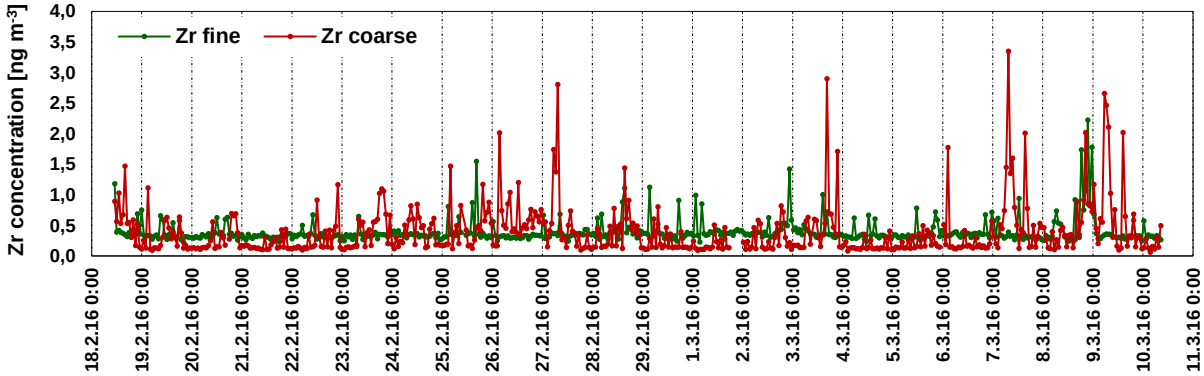

Figure S23: Hourly concentrations (ng m^{-3}) of Zr measured in the fine (green) and coarse (red) fractions.

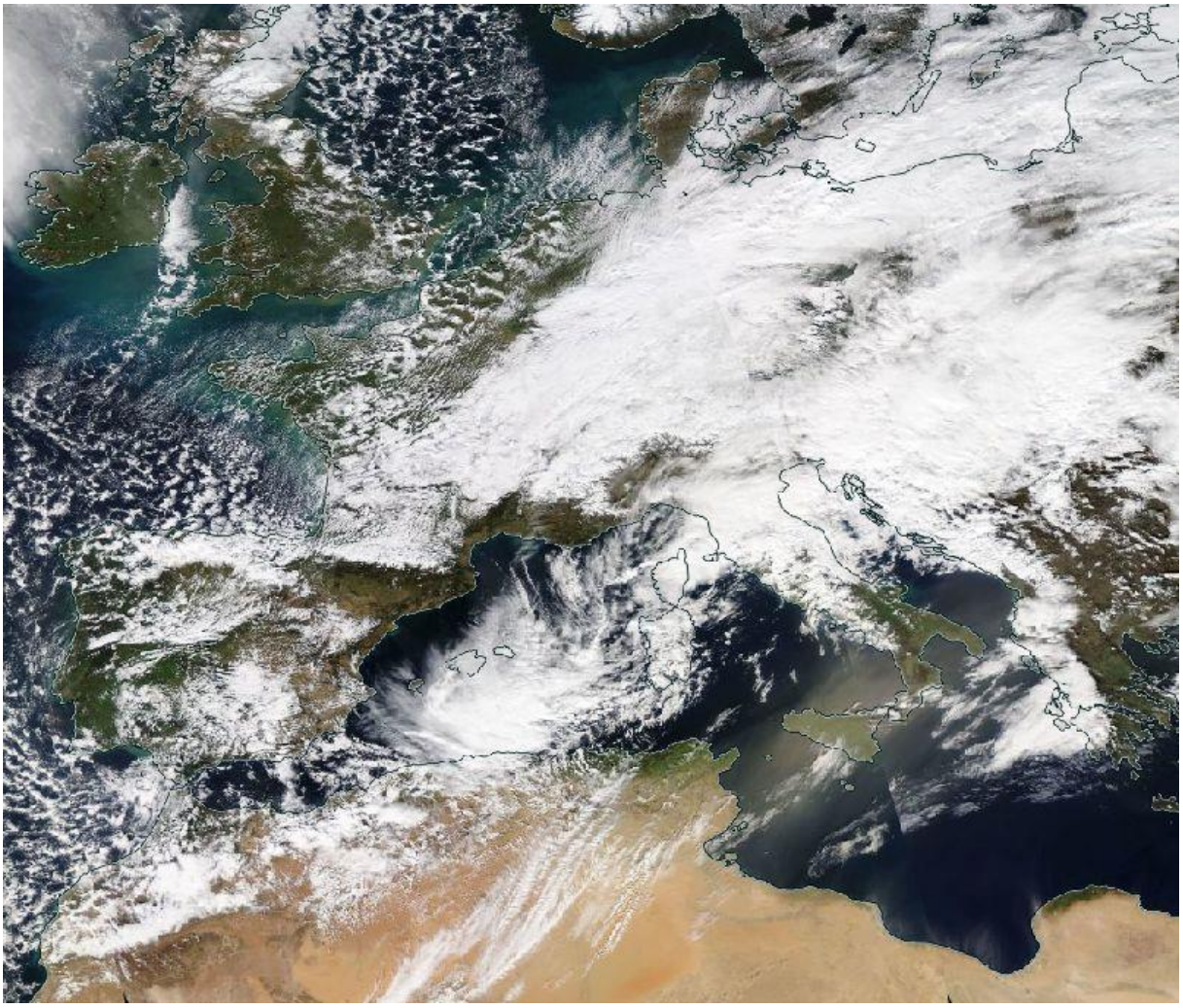

Figure S24: Aqua MODIS corrected reflectance (true color) on 15 February, 2016. NASA EOSDIS Worldview (https://worldview.earthdata.nasa.gov/).

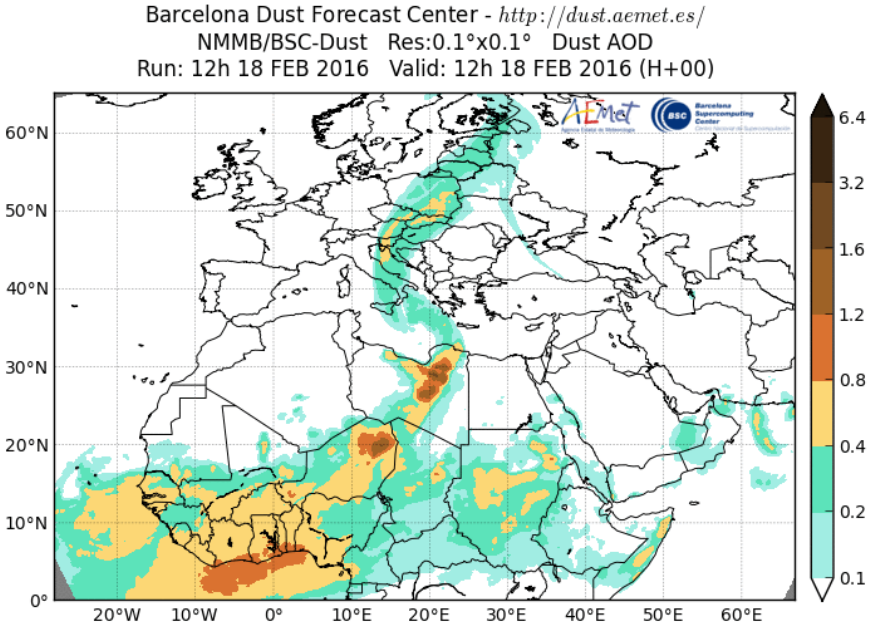

Figure S25: Aerosol Optical Depth (AOD) forecast for 18 February, 12 UTC. Image from the NMMB/BSC-Dust model operated by the Barcelona Supercomputing Center, Spanish National Supercomputing Center (https://www.bsc.es/ess/bsc-dust-daily-forecast/).

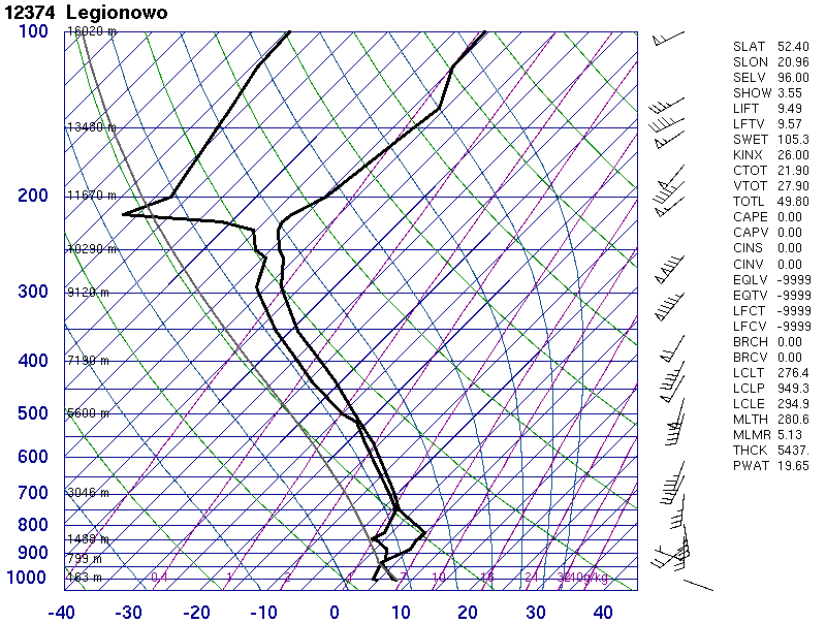

Figure S26: Skew T-log p diagrams for Legionowo on 18 February, 12 UTC. University of Wyoming (http://weather.uwyo.edu/upperair/sounding.html).